Published in final edited form as:
Acc Chem Res. 2009 January 20; 42(1): 193–203. doi:10.1021/ar8001409.

Small-Molecule Fluorescent Sensors for Investigating Zinc Metalloneurochemistry

Elizabeth M. Nolan and **Stephen J. Lippard**
Department of Chemistry, Massachusetts Institute of Technology, Cambridge, MA 02139

Conspectus

Metal ions are involved in many neurobiological processes relevant to human health and disease. The metalloneurochemistry of Zn(II) is of substantial current interest. Zinc is the second most abundant d-block metal ion in the human brain and its distribution varies, with relatively high concentrations found in the hippocampus. Brain zinc is generally divided into two categories: protein-bound and loosely-bound. The latter pool is also referred to as histochemically observable, chelatable, labile, or mobile zinc. The neurophysiological and neuropathological significance of such mobile Zn (II) remains enigmatic. Studies of Zn(II) distribution, translocation, and function in vivo require tools for its detection. Because Zn(II) has a closed-shell d^{10} configuration and no convenient spectroscopic signature, fluorescence is a suitable method for monitoring Zn(II) in biological contexts.

This Account summarizes work by our laboratory addressing the design, preparation, characterization, and use of small-molecule fluorescent sensors for imaging mobile Zn(II) in living cells and samples of brain tissue. These sensors provide “turn-on” or ratiometric Zn(II) detection in aqueous solution at neutral pH. By making alterations to the Zn(II)-binding unit and fluorophore platform, we have devised sensors with varied photophysical and metal-binding properties. We used several of these probes to image Zn(II) distribution, uptake, and mobilization in a variety of cell types, including neuronal cultures. Goals for the future include developing strategies for multi-color imaging, further defining the quenching and turn-on mechanisms of the sensors, and employing the probes to elucidate the functional significance of Zn(II) in neurobiology.

Introduction

“Metalloneurochemistry” defines a field at the intersection of inorganic chemistry and neuroscience and includes explorations of metal ions as neurotransmitters, as co-factors in neuroproteins, and as neurotoxins.[1] Most early investigations of metal ions in the central nervous system focused on the neuromodulatory roles of K(I) and Ca(II). The importance of d-block metals, including Mn(II), Fe(II), Cu(II), and Zn(II), in neurobiology has emerged recently.[2,3] We are primarily interested in Zn(II), the second most abundant d-block metal ion in the human brain.[4] In certain substructures of the mammalian hippocampus, “mobile” Zn(II) is co-localized with glutamate in presynaptic vesicles.[5] This Zn(II) pool has been implicated in both neurophysiology and disease, but details of its functional significance remain unclear.[6-8] Some questions include: (i) Is Zn(II) a neurotransmitter? (ii) What factors govern Zn(II) release into the synapse[9-12] in physiological and pathological contexts? (iii) What ligands coordinate vesicular and synaptic Zn(II)? (iv) How and why does Zn(II) influence signaling cascades and synaptic plasticity? Studies of these phenomena require a combination of chemistry, biology, electrophysiology, and optical imaging. To facilitate such investigations, we initiated a program in Zn(II) sensor design, largely inspired by prior work in Ca(II)

Correspondence: Email: lippard@mit.edu, Phone: 617-253-1892, Fax: 617-258-8150 .

detection.[13] This Account summarizes studies from our laboratory to date addressing the design, characterization, and use of small-molecule fluorescent sensors for imaging Zn(II) in vivo.

Zn(II) Sensor Design

There are many criteria for a fluorescent Zn(II) sensor that operates in biological samples.[14] It must be selective for Zn(II) over all other constituents in the biological milieu, including millimolar concentrations of Na(I), K(I), Ca(II), and Mg(II), and provide Zn(II) detection with spatial and temporal resolution. The probe affinity, measured by its dissociation constant (K_d), should approach the median concentration of Zn(II) in the sample for monitoring its flux. Other desirable characteristics include rapid and reversible Zn(II) coordination, excitation and emission wavelengths in the visible/near-IR/IR regions for single photon excitation, a bright (Φ x ε) signal, water-solubility, non-toxicity, and photostability. Depending on the application, either an intracellular or an extracellular probe might be required, which necessitates firm understanding of sensor uptake and distribution in cells.

Many strategies have been reported for turn-on and ratiometric Zn(II) sensors.[15-18] Our approaches have largely focused on the fluorescein platform. Fluorescein has excellent photophysical properties ($\Phi \sim 1$, $\varepsilon \sim 70{,}000\ M^{-1}cm^{-1}$ at pH 7), is compatible with the 488 nm Ar laser line and commercially available filter sets, and is commonly used as a biological marker. We initially incorporated amine-based chelates at the 4′ and 5′ positions of the "top" xanthenone unit of the fluorescein, a design feature analogous to that of Calcein,[19] which we hypothesized would quench fluorescein emission via photoinduced electron transfer (PET).[20] Because Zn(II) has a closed-shell d^{10} electronic configuration, we anticipated that its coordination would alleviate PET and provide fluorescence "turn-on." Although turn-on behavior is frequently observed, empirical data indicate that a simple PET mechanism whereby an amine lone pair electron quenches fluorescein emission is insufficient to describe the photophysical properties of the probes described herein.

We first reported ZP1 and ZP2 (Figure 1).[21,22] These high-affinity (sub-nM) Zn(II) chelates employ the di(2-picolyl)amine (DPA) ligand, afford fluorescence turn-on upon Zn(II) coordination, and operate in the biological milieu. They provided a foundation for the design of new probes with other desirable attributes. We subsequently prepared Zn(II) sensors that (i) spanned a wide range of K_d values, (ii) exhibited improved Zn(II) selectivity and Zn(II)-specific fluorescence turn-on, (iii) displayed improved photophysical properties, and (iv) coordinated Zn(II) rapidly and reversibility on the millisecond timescale. Our approach was to systematically modify the fluorophore and Zn(II)-binding units.

Zinpyr Sensors

Symmetrical Zinpyr

The Zinpyr family **1-20** contains fluorescein-based sensors with DPA or DPA-derived chelates (Figure 1).[21-29] ZP1-2 fluoresce brightly in their Zn(II)-bound forms ($\Phi_{Zn} \geq 0.87$), but also display relatively high background fluorescence ($\Phi_{free} \geq 0.25$, Table S1, Supporting Information) and exhibit proton-induced turn-on. From pH-dependent titrations monitored by fluorescence, which show emission enhancement when moving from pH ~10 to ~5, the Φ_{free} values were attributed to protonation of the tertiary amine at physiological pH.* Derivatives **3-7** were prepared to determine whether electronegative substitution would reduce

*The pK_a and K_d values reported and discussed here are derived from fluorescence titrations, which provide a means to evaluate sensor behavior for practical applications. They do not reveal all protonation or Zn(II) coordination events, however. Potentiometric titrations provide a more comprehensive assessment of pK_a and K_d values (B. A. Wong and S. J. Lippard, manuscript in preparation).

Φ_{free}.[23] Fluorination at the 2′ and 7′ positions afforded ZP3, which has ~2.5-fold less background fluorescence than ZP1 (Φ_{free} = 0.15, Table S1).[23] Halogenation, and particularly fluorination, of the benzoate moiety reduced both Φ_{free} and Φ_{Zn} values relative to ZP1. The latter effect results in ~2-fold or less dynamic range. The pK_a associated with fluorescence enhancement upon protonation decreases somewhat as X = H > Cl > F (Table S1). This trend occurs because the titration curves for ZP1/ZP3 are shifted to lower pH relative to ZP2, behavior analogous to that observed for ZS5-7 (*vide infra*, Figure 2), and fluorescein and its chlorinated and fluorinated analogs.[30,31] Background fluorescence reduction also accompanies fluorination of ZnAFs, which are pH insensitive in the physiological range,[32] and for a fluorinated thioether-containing sensor ZS2, which has a comparable pH-dependent emission profile to its chlorinated analog (*vide infra*, Figure 2). From these observations, we conclude that 2′,7′-difluorofluorescein affords sensors with lower Φ_{free} for reasons in addition to protonation.

ZP **1-7** form 1:1 and 1:2 ZP:Zn(II) complexes with fluorescent-derived K_d values for Zn(II) of 0.5 - 1.1 nM. X-ray crystallographic characterization of the 1:2 ZP1:Zn(II) complex revealed distorted trigonal bipyramidal geometry at both Zn(II) centers, each being coordinated by the three nitrogen atoms of a DPA moiety, the phenolic oxygen atom of DCF, and a water molecule (Figure 3).[22] Stopped-flow kinetic investigations of ZP1 and ZP3 demonstrated rapid Zn(II) coordination ($k_{on} > 106\ M^{-1}s^{-1}$) and slow dissociation ($k_{off} < 3 \times 10^{-3}\ s^{-1}$) at room temperature (Table S2, Figure 4).[32] Because of the DPA moiety, **1-7** bind Mn(II), Fe(II), Co(II), Ni(II), and Cu(II) with high affinity. These paramagnetic ions effectively quench the basal fluorescence of symmetrical ZP and, excluding Mn(II), interfere with Zn(II)-induced fluorescence enhancement. ZP turn-on occurs in the presence of Cd(II) and, in some instances, Hg(II).

ZP1 and ZP3 readily permeate live cells, as expected based on their TPEN-like structures, and are Zn(II)-responsive in vivo. To provide extracellular ZP, ZP1 analogs **8-9** with a carboxylate group at the 5′ or 6′ position were prepared (Figure 1).[24] These probes have similar photophysical and metal-binding properties as **1-7** (Table S1) and do not permeate cultured cells. Installation of an ethyl ester moiety afforded “trappable” forms **10-11** that enter cells and are retained following hydrolysis by an esterase.

To reduce the binding affinity, ZP1 analogs **12-13** with methylated pyridine rings were synthesized (Figure 1).[28] Me_2ZP1 and Me_4ZP1 exhibit K_d values for Zn(II) of 3.3 ± 0.2 nM and 0.63 ± 0.05 μM, respectively, and provide ~4- and ~2.5-fold fluorescence enhancement (Table S1). Me_4ZP1 is selective for Zn(II) over Fe(II), which may be significant for biological work; failure of Fe(II) homeostasis has been correlated with several neuropathologies.[33] Because ZP1 and Me_nZP1 have comparable photophysical properties, they provide a suite of probes for exploring Zn(II) concentrations in the sub-nM to low-μM range. Additional elevation of the Zn(II) K_d value into the ~10 - 100 μM range was achieved by removing a pyridyl group from an arm on each DPA unit of ZP1 or Me_2ZP1 to afford ZAP1/3 or ZAP2 (**21-23,** Figure 1), but these compounds have high background fluorescence and provide no Zn (II)-induced turn-on at neutral pH (Table S1).[35] These observations indicate that the entire ligand appendage, not just the tertiary amine nitrogen atom, contributes to fluorophore quenching.

Asymmetrical Zinpyr

ZP4-8 employ asymmetrical fluorescein platforms (**14-18**, Figure 1).[25-27] They each contain a single DPA-derivatized aniline as the metal-binding group. Because aniline has a lower pK_a value than a tertiary amine, we initially hypothesized that its use would afford reduced pH-dependent background fluorescence at physiological pH relative to that of ZP1.[25] Indeed, ZP4 exhibits lower background fluorescence (Φ_{free} = 0.06) than symmetrical ZP. Zn(II)

coordination gives ~6-fold turn-on (Φ_{Zn} = 0.34).[25] The Φ_{Zn} value indicates that Zn(II) coordination does not fully restore fluorescein emission. ZP5-7 were subsequently prepared to determine whether substitution para to the aniline nitrogen atom (X = F, Cl, OMe) would tune background fluorescence.[26] Photophysical characterization revealed behavior that did not correlate with the relative electron-donating or -withdrawing nature of the substituent (Table S1), indicating a more complicated paradigm. Background fluorescence reduction (Φ_{free} = 0.03) and ~12-fold fluorescence enhancement was achieved with fluorinated ZP8.[27] ZP4-8 all form 1:1 ZP:Zn(II) complexes and exhibit sub-nM K_d values for Zn(II). X-ray crystallographic characterization of a salicylaldehyde-based ZP4:Zn(II) model indicated distorted octahedral geometry with the sixth position occupied by a water molecule.[25] The metal ion selectivity profiles are like those of symmetrical ZP, but coordination of paramagnetic metals to asymmetric ZP causes only negligible fluorescence turn-off because the apo sensors are already substantially quenched.

Modification of the DPA appendage of ZP4 to include pyrrole moieties provided ZP9 and ZP10 (**19**-**20**, Figure 1).[29] Pyrrole and *N*-methypyrrole, poor bases and weakly or non-coordinating heterocycles at neutral pH, were chosen to raise the dissociation constant relative to those of ZP1-8. Their photophysical properties are similar to those of ZP4 with ~12 (ZP9) and ~7-fold (ZP10) emission enhancement and $\Phi_{Zn} > 0.30$ (Table S1). Job plot analyses indicated 1:1 ZP:Zn(II) coordination and titrations provided Zn(II) K_d values of 0.69 ± 0.4 μM (ZP9) and 1.9 ± 0.2 μM (ZP10). A combination of ZP4, ZP9, and ZP10 therefore provides a sensor collection for detecting sub-nM to low-μM Zn(II) concentrations. The k_{on} values for Zn(II) association are comparable to those of DPA-containing ZP, and ZP9-10 exhibited more rapid Zn(II) dissociation ($k_{off} > 1\ s^{-1}$) (Table S2). ZP9-10 are selective for Zn(II) over Fe(II) and Cd (II).

To ascertain the contribution of the aniline unit to fluorescence quenching in ZP4-10, we prepared an aniline-functionalized fluorescein.[29] Its Φ value of 0.06 indicates that the aniline moiety itself is responsible for quenching fluorescein. Although the pK_a values corresponding to an increase in fluorescence moving from high to low pH of ZP4-8 and ZP1-3 generally overlap, the asymmetric probes exhibit significantly less proton sensitivity. In general, ≤2-fold fluorescence enhancement occurs for ZP4-8/ZS4 compared to >20-fold for symmetric ZP/ZS when the pH is lowered from ~12 to ~5 (Figure 2, top). These features, and the low Φ_{Zn} values, suggest a separate, and not yet defined, quenching mechanism for aniline-containing probes.

Zinspy Sensors

The Zinspy (ZS) sensors **24**-**33** have sulfur moieties in the Zn(II)-binding unit (Figure 5).[36, 37] This work began by exploring zinc-thiolate linkages, inspired by the Cys_2His_2 binding motif of Zn(II) finger peptides. Sensors with more poorly coordinating thioether and thiophene groups proved to be better for turn-on Zn(II) fluorescence. Zinspy probes display lower Zn(II) affinity and improved Zn(II) selectivity relative to ZP1-8.

ZS1-4 contain pyridyl-amine-thioether ligands (**24**-**27**, Figure 5).[35] Because thioethers have relatively low affinity for Zn(II) compared to nitrogen and oxygen donors, we reasoned that incorporation of this group into the chelate would raise the Zn(II) K_d value and modulate Zn (II) selectivity relative to ZP. ZS1 and ZS2 provide modest ~1.4 and ~2-fold fluorescence turn-on with Zn(II) addition (Table S1) and are also sensitive to protons (Figure 2). A comparison of ZP1/ZS1 and ZP3/ZS2 reveals that the thioether-for-pyridyl substitution increases Φ_{free} and decreases Φ_{Zn}, a trend like that observed for ZP1/ZAP1. ZS3, an asymmetrical tertiary amine probe, displays high background fluorescence (Φ_{free}= 0.73) and gives no turn-on. The diminished fluorescence quenching resulting from substitution of fluorescein with one tertiary amine-based chelate (ZS3) instead of two (ZS1) indicates that both ligand groups contributed

to quenching of the fluorescein photoexcited state. ZS4 provides fluorescence behavior like that of its DPA analog ZP4 (Table S1); however, the Zn(II) complex is not water-soluble. ZS1, ZS2, and ZS4 are selective for Zn(II) over Fe(II) and also turn on with Cd(II). Excess Zn(II) was required to achieve full fluorescence enhancement with ZS1-2, indicating lower Zn(II) affinity relative to ZP1.

We subsequently worked to improve the dynamic range and maintain the Zn(II) binding properties of ZS1-4. Based on observations from ZP1/ZAP/ZS and a study that suggested groups distant to a fluorophore contribute to quenching,[38] we hypothesized that replacement of the thioether with an aromatic heterocycle would reduce Φ_{free} and provide and greater fluorescence enhancement following Zn(II) coordination. We therefore substituted the ZS thioether moiety with a thiophene.[37]

Comparison of ZS5-7 (**28-33**, Figure 5) with ZS1-2 reveals that introduction of a thiophene group lowers Φ_{free} and affords up to ~4-fold turn-on (Table S1). This trend is particularly evident for the ZS2/ZS7 pair where Φ_{free} decreases from 0.39 to 0.25. As a result, the quantum yields and dynamic ranges of ZS5-7 more closely resemble those of the ZP family, although Φ_{free} is generally higher and indicates that DPA quenches the fluorescein excited state more effectively than the pyridyl-amine-thiophene unit.

Thiophene-containing ZS provides maximum fluorescence turn-on in the presence of ~10 to ~50 equiv of Zn(II), depending on fluorescein halogenation. The K_d value of ZS5 for Zn(II) is 1.5 ± 0.2 μM and it increases with fluorination of the xanthenone and benzoate moieties (K_d = 3.7 - 5.0 μM, Table S2). We attribute this trend to reduction in electron density on the oxygen atom upon fluorination, making it a relatively poor donor and weakening the Zn—O bond. X-ray crystallographic studies employing a salicylaldehyde-based ZS5 model confirmed that the thiophene does not coordinate Zn(II). The selectivity of ZS5-7 follows that of ZS1-4 with a preference for Zn(II) over Fe(II). ZS5 and its congeners are also selective for Zn(II) over Hg(II). Kinetic investigations revealed that ZS bind Zn(II) rapidly and reversibly ($t_{1/2}$ > 50 msec) (Table S2, Figure 4).

QZ Sensors

QZ1 and QZ2 are fluorescein-based dyes containing one or two 8-aminoquinoline units (**34-35**, Figure 6).[33] We anticipated that the combination of quinoline, employed in TSQ and related probes,[39,40] and fluorescein would provide bright sensors with lower Zn(II) affinity than ZP/ZS family members. QZ1 is asymmetrical and therefore analogous to ZP4, but provides ~42-fold fluorescence enhancement upon Zn(II) addition (Φ_{free} = 0.024; Φ_{Zn} = 0.78, Table S1). We subsequently prepared QZ2. Because, in the ZS1/ZS3 couple, attachment of two metal-binding groups reduces Φ_{free} relative to only one, we reasoned that QZ2 would exhibit even greater dynamic range. Indeed, QZ2 provides ~150-fold turn-on following Zn(II) coordination, with Φ_{free} = 0.005. This value is comparable to Φ_{free} for some benzoate-substituted ZnAF dyes[31] and represents an ~76-fold reduction in background fluorescence relative to ZP1 (Figure 7).

Job plot analysis indicated that QZ1 forms a 1:1 complex with Zn(II). A K_d value of 33 ± 2 μM was obtained by fluorimetric titration. A K_d value of 41 ± 3 μM was obtained for QZ2 from stopped-flow studies. These data indicate that both Zn(II) coordination events enhance QZ2 fluorescence. QZ display rapidly reversible Zn(II) coordination with $t_{1/2}$ < 0.5 ms (Table S2, Figure 4). The turn-on of QZ is Zn(II)-selective; only Ni(II) and Cu(II) interfere with the Zn(II) response.

Porphyrin-Based Sensor

As part of an initiative to prepare MRI Zn(II) sensors, we synthesized the DPA-substituted porphyrin $(DPA\text{-}C_2)_2$-$TPPS_3$ ($TPPS_3$, 5-phenyl-10,15,20-tris(4-sulfonatophyenyl)porphine) (**36**, Figure 8).[41] $(DPA\text{-}C_2)_2$-$TPPS_3$ emits (Φ_{free} = 0.004) in the far-red (648 nm) and near-IR (715 nm) regions following excitation into its Soret band (λ_{ex} = 418 nm) at neutral pH. Addition of Zn(II) to $(DPA\text{-}C_2)_2$-$TPPS_3$ provides >10-fold fluorescence enhancement (Φ_{Zn} = 0.046) (Figure 9). The Zn(II) selectivity of $(DPA\text{-}C_2)_2$-$TPPS_3$ (K_d = 12 nM) parallels that of ZP1. The optical properties of $(DPA\text{-}C_2)_2$-$TPPS_3$ are ideal for biological imaging applications; the long-wavelength emission avoids autofluorescence from native biomolecules. $(DPA\text{-}C_2)_2$-$TPPS_3$ permeates and responds to elevated Zn(II) levels in live cells.

Ratiometric Sensors

Ratiometric detection, which compares fluorescence intensity ratios at two different wavelengths before and after analyte recognition, is another approach to Zn(II) sensing. To date, relatively few small-molecule ratiometric Zn(II) probes are available.[18]

We considered three strategies for ratiometric Zn(II) detection.[42-44] Our first approach employed a hybrid fluorescein-rhodamine platform with a cyclen receptor (**37**, RF2, Figure 10), which we anticipated would shift between iminophenoxy (rhodamine-like) and aminoquinone (fluorescein-like) mesomers following Zn(II) coordination.[42] RF2, however, provides no ratiometric response and only weak fluorescence turn-on following Zn(II) coordination. This behavior was attributed to protonation of the macrocycle at neutral pH and adoption of the aminoquinone mesomer in its apo and Zn(II)-bound forms.

ZP1 and ZP4 provided good starting points for ratiometric Zn(II) detectors. The seminaphthofluorescein analog of ZP4, ZNP1 (**38**, Figure 10), affords single-excitation dual-emission ratiometric Zn(II) detection (λ_{624} / λ_{524}) when excited at 499 nm.[44] The ~18-fold ratio change results from selective enhancement of the 624 nm emission band (Figure 11). In this sense, ZNP1 is fundamentally a turn-on Zn(II) sensor. Because of the conserved aniline-based ligand, ZNP1 exhibits similar Zn(II) affinity (K_d = 0.50 nM) and selectivity as ZP4. ZNP1 was used for ratiometric imaging of Zn(II) release in COS7 cells.

Dual-excitation dual-emission ratiometric detection of Zn(II) was achieved by linking a Zn (II)-insensitive coumarin 343 to ZP1 through an alkyl-amidoester (CZ1) or diester (CZ2) linkage (Figure 12).[43,45] CZ weakly emit (Φ_{free} < 0.05) at pH 7. Hydrolysis of the ester bonds by pig liver esterase in vitro enhances emission from both the ZP1 and coumarin chromophores with ~8-(CZ1) and ~4-fold (CZ2) increases in the ratio of ZP1/coumarin emission after Zn(II) addition. These sensors are cell permeable. A ratiometric change occurs in HeLa cells treated with CZ2 and Zn(II)/pyrithione.

Principles Derived from Fluorescein-Based Sensors

We draw several generalizations about sensor behavior that may be applied to the design of future probes.

We consider first the fluorescent properties of ZP, ZS and QZ, dividing them into three categories defined by the nature of the metal-binding unit: tertiary amine, aniline or quinoline. Sensors with tertiary amine-based chelates are generally more emissive than those with aniline in both free and Zn(II)-bound forms. The comparison indicates the tertiary amine unit to be a less efficient quencher than aniline. Moreover, aniline protonation results in only modest fluorescence enhancement and Zn(II) coordination fails to restore full fluorescein-like emission (typically Φ_{Zn} < 0.4). Such observations define a role for the aniline π system in

fluorescence quenching. The QZ sensors, which have aniline-like linkages, have proton sensitivity similar to that of ZP4-10 and exhibit much higher quantum efficiencies in their Zn (II)-bound forms. Zn(II) binding to QZ directly perturbs the quinoline π system through coordination to the ring heteroatom, and we speculate that the enhanced turn-on may originate from this feature. The photophysics of these sensors is complex and awaiting mechanistic investigation. In addition to PET, internal charge transfer (ICT) may contribute to the fluorescence behavior of the xanthenone-based sensors because they have phenolic oxygen atoms in the metal-binding units.[46]

Comparison of the tertiary amine and aniline-based systems indicates that the emission properties of the former are more sensitive to variations in the donor arms. By contrast, variations of the donor arms in aniline-based systems have little effect on sensor emission. Another observation is the difference between one versus two metal-binding units. The latter sensors exhibit lower background fluorescence than their asymmetrical analogs. From our studies thus far, we find that obtaining a reasonable Φ_{free} value at neutral pH for xanthenone-substituted fluoresceins employing tertiary amine switches is facilitated by the presence of ligand appendages at both the 4′ and 5′ positions with two aromatic heterocycles in each metal-binding unit.

Substitutions on the fluorescein platform also impact the emission profiles. Substitution of the benzoate moiety with halogens or carboxylates results in diminished Φ_{free} and Φ_{Zn} values. Halogenation tunes excitation and emission wavelengths over a small (~35 nm), but potentially useful, range.

Ligand modifications provide varied Zn(II) binding affinity, association and dissociation rates, and selectivity. Reducing the number of donor atoms raises the apparent K_d of the Zn(II) complexes to the sub- and mid-μM range. More subtle modifications are required to obtain sensors with dissociation constants in the low- to mid-nM range, such as methylation of DPA. Fluorescein halogenation also tunes the Zn(II) affinity, with xanthenone and benzoate substitution raising the apparent K_d value relative to probes based on unsubstituted fluorescein. All sensors described in this work coordinate Zn(II) rapidly and, in some cases, reversibly. Departure from the DPA binding motif by substitution of one pyridyl donor with an alternative group has little effect on the Zn(II) association rate and affords faster Zn(II) dissociation. The QZ ligand system affords the most rapid and reversible Zn(II) binding.

Metal ion selectivity experiments reveal the degree to which a given sensor is Zn(II)-selective, for such a fluorescence response is critical for biological work. All of the Zn(II) probes discussed in this work specifically coordinate Zn(II) at physiological concentrations of K(I), Na(I), Ca(II), and Mg(II), demonstrating that this selectivity is easy to maintain with metal-binding units comprising multiple nitrogen and sulfur atoms. Coordination of tertiary-amine-based sensors to Fe(II), Co(II), Ni(II), and Cu(II) always results in immediate and substantial fluorescence quenching. When aniline- and quinoline-based sensors chelate these particular metal ions, there is little or no effect on emission because the sensors are substantially quenched in their metal-free forms. The selectivity of a given probe for the Group 12 congeners obey the hard/soft acid/base principle whereby sensors with nitrogen-rich chelates preferentially coordinate to Zn(II) and those with a thioether group bind Hg(II) more tightly. Substitution of one pyridyl group from the DPA unit with another moiety routinely conveys selectivity for Zn (II) over Fe(II). The selectivity for Zn(II) over Co(II) in the QZ systems is unique. Explanations of such behavior will be aided by further solution studies and crystallographic characterization of the fluorescein-metal complexes.

Biological Imaging Applications

Our long-term goal is to employ sensors to elucidate mechanisms of Zn(II) mobilization, trafficking, and signaling in neurobiology. We have therefore studied several Zn(II) sensors in living cells and brain tissue. Our approach is first to determine whether a sensor is cell permeable, stable, Zn(II) responsive and reversible in immortalized cells and, subsequently, in primary neuronal cultures from rat. Mixtures of Zn(II) and pyrithione, a cell-permeable ionophore, are employed to deliver exogenous Zn(II) to the cells, and *N',N',N",N"*-tetrakis(2-picolyl)ethylenediamine (TPEN) is a cell-permeable metal ion chelator used in reversibility studies. Next, we determine whether endogenous Zn(II) can be imaged. We routinely examine two models for endogenous Zn(II): (i) acute hippocampal slices from adult rat, which contain histochemically observable Zn(II) in the dentate gyrus (DG) and CA3 regions, and (ii) stimulated Zn(II) release from native intracellular stores. Our studies reveal some general principles about Zn(II) sensor structure and behavior in cells. Tertiary amine-based probes (ZP3, ZS5) are more readily cell permeable than aniline-based ones (ZP4, QZ2), assuming no carboxylate substitution on the benzoate moiety. Alternations of the Zn(II)-binding unit confer variable intracellular localization, and the relative binding affinities can be employed to report on varying intracellular Zn(II) concentrations.

Following initial studies of ZP1, which revealed intracellular Golgi-associated staining,[22] we focused on probes with greater dynamic range. We extensively characterized ZP3 and ZS5 in vivo; they are versatile intracellular Zn(II) imaging agents. ZP3 exhibits Zn(II)-induced turn-on following treatment of HEK cells and cultured DG neurons with S-nitrocysteine (SNOC), and it provides vivid staining of the Zn(II)-rich DG and CA3 regions of hippocampal slices from adult rat (Figure 13).[23] ZS5 also responds to SNOC-induced Zn(II) availability in DG neurons (Figure 14) and was employed to monitor glutamate-mediated Zn(II) uptake in hippocampal neurons.[37] Colocalization studies in HeLa cells showed that ZP3, like ZP1, sequesters in the Golgi whereas ZS5 localizes to mitochondria (Figure 15).[37] The origin of Zn (II) sensor sequestration in different subcellular organelles as a result of structural modification is unclear, but may reflect different protein association. Once understood, this phenomenon may be advantageous for studies of Zn(II) trafficking.

One synthetic goal has been to prepare sensors with varying Zn(II) affinities to monitor Zn(II) concentrations in cells. We therefore compared the response of ZP3 (sub-nM K_d) and QZ2 (μM K_d) to a range of exogenously introduced Zn(II) concentrations in HeLa cells (Figure 16).[33] ZP3 fluorescence saturates before that of QZ2, reflecting the relative probe affinity for Zn (II) in cells. Lower-affinity sensors can be employed in cells to report on relatively high concentrations of analyte.

Cytotoxicity is a potential side effect when treating live cells with a probe. Although we have not seen evidence for cytotoxic effects during imaging experiments, most of our work required short incubation periods up to several hours. We therefore investigated the consequences of more extended sensor treatment on cell viability by conducting cytotoxicity assays in HeLa cells. The IC_{50} values of ZP1 (2.3 ± 0.5 μM), ZP3 (4.3 ± 0.8 μM) and ZPF1 (3.0 ± 0.6 μM), determined five days following continuous exposure to the sensors by the colorimetric MTT assay indicated that sub- and low-μM concentrations of ZP are essentially non-toxic and can be used for biological studies that require prolonged exposure times (Figure 17; MTT is 3-(4,5-dimethylthiazol-2-yl)-2,5-diphenyltetrazolium bromide).

Summary and Outlook

Our synthetic efforts have provided a collection of Zn(II) sensors with (i) K_d values that cover approximately six orders of magnitude; (ii) Zn(II)-selective fluorescence enhancement, binding Zn(II) over many other divalent metal ions and biologically relevant cations; (iii) up

to ~150-fold fluorescence enhancement; (iv) rapid and reversible Zn(II) coordination with association and dissociation rates on the biological timescale. Some of these Zn(II) sensors were successfully applied in biological contexts. Nevertheless, challenges remain. Although we have guiding principles for designing fluorescein-based turn-on sensors, the molecules are complex and their quenching mechanisms are not yet defined. A theoretical understanding would be helpful for further rational design. Strategies for multi-color imaging and site-specific sensor attachment are especially warranted for biological investigations. Ultimately, the most important goal for the future is to apply Zn(II) sensors to elucidate the details of physiological signaling by and pathological mobilization of the ion in neurobiology. Such an achievement will provide the ultimate justification of the effort expended to design, synthesize and characterize the expanded family of zinc sensors.

Supplementary Material

Refer to Web version on PubMed Central for supplementary material.

Acknowledgements

Work on Zn(II) sensing in our laboratory is supported the National Institute of General Medical Sciences. We thank Brian A. Wong for insightful discussions.

Biography

Biographical Information

Elizabeth M. Nolan received her B.A. in Chemistry from Smith College. She joined Professor Stephen J. Lippard's group at MIT and received her Ph.D. in 2006. Liz is a post-doctoral fellow in Professor Christopher T. Walsh's laboratory at Harvard Medical School.

Stephen J. Lippard graduated from Haverford College with a B.A. in Chemistry and received his Ph.D. from the Massachusetts Institute of Technology. He served on the faculty of Columbia University and is currently the Arthur Amos Noyes Professor of Chemistry at MIT.

References

(1). Burdette SC, Lippard SJ. Meeting of the Minds: Metalloneurochemistry. Prod. Nat. Acad. Sci. USA 2003;100:3605–3610.

(2). Burdette SC, Lippard SJ. Coordination Chemistry for the Neurosciences. Coord. Chem. Rev 2001;216-217:333–361.

(3). Que EL, Domaille DW, Chang CJ. Metals in Neurobiology: Probing their Chemistry and Biology with Molecular Imaging. Chem. Rev 2008;108:1517–1549. [PubMed: 18426241]

(4). Frederickson CJ. Neurobiology of Zinc and Zinc-Containing Neurons. Int. Rev. Neurobiol 1989;31:145–238. [PubMed: 2689380]

(5). Salazar G, Craige B, Love R, Kalman D, Faundez V. Vglut1 and ZnT3 Co-targeting Mechanisms Regulate Vesicular Zinc Stores in PC12 Cells. J. Cell. Sci 2005;118:1911–1921. [PubMed: 15860731]

(6). Choi DW, Koh JY. Zinc and Brain Injury. Annu. Rev. Neurosci 1998;21:347–375. [PubMed: 9530500]

(7). Takeda A. Zinc Homeostasis and Functions of Zinc in the Brain. Biometals 2001;14:343–351. [PubMed: 11831464]

(8). Frederickon CJ, Koh J-Y, Bush AI. The Neurobiology of Zinc in Health and Disease. Nature Rev. Neurosci 2005;6:449–462. [PubMed: 15891778]

(9). Assaf SY, Chung S-H. Release of Endogenous Zn^{2+} from Brain Tissue During Activity. Nature 1984;308:734–736. [PubMed: 6717566]

(10). Howell GA, Welch MG, Frederickson CJ. Stimulation-Induced Uptake and Release of Zinc in Hippocampal Slices. Nature 1984;308:736–738. [PubMed: 6717567]

(11). Kay AR. Evidence for Chelatable Zinc in the Extracellular Space of the Hippocampus, But Little Evidence for Synaptic Release of Zn. J. Neurosci 2003;23:6847–6855. [PubMed: 12890779]

(12). Qian J, Noebels JL. Visualization of Transmitter Release with Zinc Fluorescence Detection at the Mouse Hippocampal Mossy Fibre Synapse. J. Physiol 2005;566:747–758. [PubMed: 15919713]

(13). Takahashi A, Camacho P, Lechleiter JD, Herman B. Measurements of Intracellular Calcium. Physiol. Rev 1999;79:1089–1125. [PubMed: 10508230]

(14). Kimura E, Koike T. Recent Development of Zinc-Fluorophores. Chem. Soc. Rev 1998;27:179–184.

(15). Kikuchi K, Komatsu K, Nagano T. Zinc Sensing for Cellular Application. Curr. Opin. Chem. Biol 2004;8:182–191. [PubMed: 15062780]

(16). Jiang P, Guo Z. Fluorescent Detection of Zinc in Biological Systems: Recent Development on the Design of Chemosensors and Biosensors. Coord. Chem. Rev 2004;248:205–229.

(17). Lim NC, Freake HC, Brückner C. Illuminating Zinc in Biological Systems. Chem. Eur. J 2005;11:38–49.

(18). Chang CJ, Lippard SJ. Zinc Metalloneurochemistry: Physiology, Pathology, and Probes. Met. Ions Life Sci 2006;1:281–320.

(19). Diehl H, Ellingboe JL. Indicator for Titration of Calcium in Presence of Magnesium Using Disodium Dihydrogen Ethylene Tetraacetate. Anal. Chem 1956;28:882–884.

(20). de Silva AP, Gunaratne HQN, Gunnlaugsson T, Huxley AJM, McCoy CP, Rademacher JT, Rice TE. Signaling Recognition Events with Fluorescent Sensors and Switches. Chem. Rev 1997;97:1515–1566. [PubMed: 11851458]

(21). Walkup GK, Burdette SC, Lippard SJ, Tsien RY. A New Cell-Permeable Fluorescent Probe for Zn^{2+} J. Am. Chem. Soc 2000;122:5644–5645.

(22). Burdette SC, Walkup GK, Spingler B, Tsien RY, Lippard SJ. Fluorescent Sensors for Zn^{2+} Based on a Fluorescein Platform: Synthesis, Properties and Intracellular Distribution. J. Am. Chem. Soc 2001;123:7831–7841. [PubMed: 11493056]

(23). Chang CJ, Nolan EM, Jaworski J, Burdette SC, Sheng M, Lippard SJ. Bright Fluorescent Chemosensor Platforms for Imaging Endogenous Pools of Neuronal Zinc. Chem. Biol 2004;11:203–210. [PubMed: 15123282]

(24). Woodroofe CC, Masalha R, Barnes KR, Frederickson CJ, Lippard SJ. Membrane-Permeable and -Impermeable Sensors of the Zinpyr Family and Their Application to Imaging of Hippocampal Zinc In Vivo. Chem. Biol 2004;11:1659–1666. [PubMed: 15610850]

(25). Burdette SC, Frederickson CJ, Bu W, Lippard SJ. ZP4, an Improved Neuronal Zn^{2+} Sesnor of the Zinpyr Family. J. Am. Chem. Soc 2003;125:1778–1787. [PubMed: 12580603]

(26). Nolan EM, Burdette SC, Harvey JH, Hilderbrand SA, Lippard SJ. Synthesis and Characterization of Zinc Sensors Based on a Monosubstituted Fluorescein Platform. Inorg. Chem 2004;43:2624–2635. [PubMed: 15074981]

(27). Chang CJ, Nolan EM, Jaworski J, Okamoto K-I, Hayashi Y, Sheng M, Lippard SJ. ZP8, a Neuronal Zinc Sensor with Improved Dynamic Range; Imaging Zinc in Hippocampal Slices with Two-Photon Microscopy. Inorg. Chem 2004;43:6774–6779. [PubMed: 15476377]

(28). Goldsmith CR, Lippard SJ. 6-Methylpyridyl for Pyridyl Substitution Tunes the Properties of Fluorescent Zinc Sensors of the Zinpyr Family. Inorg. Chem 2006;45:555–561. [PubMed: 16411690]

(29). Nolan EM, Jaworski J, Racine ME, Sheng M, Lippard SJ. Midrange Affinity Fluorescent Zn(II) Sensors of the Zinpyr Family: Syntheses, Characterization, and Biological Imaging Applications. Inorg. Chem 2006;45:9748–9757. [PubMed: 17112271]

(30). Leonhardt H, Gordon L, Livingston R. Acid-Base Equilibria of Fluorescein and 2′,7′-Dichlorofluorescein in Their Ground and Fluorescent States. J. Phys. Chem 1971;75:245–249.

(31). Sun W-C, Gee KR, Klaubert DH, Haugland RP. Synthesis of Fluorinated Fluoresceins. J. Org. Chem 1997;62:6469–6475.

(32). Hirano T, Kikuchi K, Urano Y, Nagano T. Improvement and Biological Applications of Fluorescent Probes for Zinc, ZnAFs. J. Am. Chem. Soc 2002;124:6555–6562. [PubMed: 12047174]

(33). Nolan EM, Jaworski J, Okamoto K-I, Hayashi Y, Sheng M, Lippard SJ. QZ1 and QZ2: Rapid, Reversile Quinoline-Derivatized Fluoresceins for Sensing Biological Zn(II). J. Am. Chem. Soc 2005;127:16812–16823. [PubMed: 16316228]

(34). Zecca L, Youdim MBH, Riederer P, Connor JR, Crichton RR. Iron, Brain Ageing and Neurodegenerative Disorders. Nat. Rev. Neurosci 2004;5:863–873. [PubMed: 15496864]

(35). Goldsmith CR, Lippard SJ. Analogues of Zinpyr-1 Provide Insight into the Mechanism of Zinc Sensing. Inorg. Chem 2006;45:6474–6478. [PubMed: 16878961]

(36). Nolan EM, Lippard SJ. The Zinspy Family of Fluorescent Zinc Sensors: Syntheses and Spectroscopic Investigations. Inorg. Chem 2004;43:8310–8317. [PubMed: 15606177]

(37). Nolan EM, Ryu JW, Jaworski J, Feazell RP, Sheng M, Lippard SJ. Zinspy Sensors with Enhanced Dynamic Range for Imaging Neuronal Zinc Uptake and Mobilization. J. Am. Chem. Soc 2006;128:15517–15528. [PubMed: 17132019]

(38). Sparano BA, Shahi SP, Koide K. Effect of Binding and Conformation on Fluorescence Quenching in New 2′,7′-Dichlorofluorescein Derivatives. Org. Lett 2004;6:1947–1949. [PubMed: 15176790]

(39). Frederickson CJ, Kasarskis EJ, Ringo D, Frederickson RE. A Quinoline Fluorescence Method for Visualizing and Assaying the Histochemically Reactive Zinc (Bouton Zinc) in the Brain. J. Neurosci. Methods 1987;20:91–103. [PubMed: 3600033]

(40). Fahrni CJ, O'Halloran TV. Aqueous Coordination Chemistry of Quinoline-Based Fluorescence Probes for the Biological Chemistry of Zinc. J. Am. Chem. Soc 1999;121:11448–11458.

(41). Zhang X, Lovejoy KS, Jasanoff A, Lippard SJ. Water-Soluble Porphyrins as a Dual-Function Molecular Imaging Platform for MRI and Fluorescence Zinc Sensing. Proc. Natl. Acad. Sci. USA 2007;104:10780–10785. [PubMed: 17578918]

(42). Burdette SC, Lippard SJ. The Rhodafluor Family. An Initial Study of Potential Ratiometric Fluorescent Sensors for Zn^{2+} Inorg. Chem 2002;41:6816–6823. [PubMed: 12470079]

(43). Woodroofe CC, Lippard SJ. A Novel Two-Fluorophore Approach to Ratiometric Sensing of Zn^{2+} J. Am. Chem. Soc 2003;125:11458–11459. [PubMed: 13129323]

(44). Chang CJ, Jaworski J, Nolan EM, Sheng M, Lippard SJ. A Tautomeric Zinc Sensor for Ratiometric Fluorescence Imaging: Application to Nitric Oxide-Induced Release of Intracellular Zinc. Prod. Natl. Acad. Sci. USA 2004;101:1129–1134.

(45). Woodroofe CC, Won AC, Lippard SJ. Esterase-Activated Two-Fluorophore System for Ratiometric Sensing of Biological Zinc. Inorg. Chem 2005;44:3112–3120. [PubMed: 15847416]

(46). Callan JF, de Silva AP, Magri DC. Luminescent Sensors and Switches in the Early 21^{st} Century. Tetrahedron 2005;61:8551–8588.

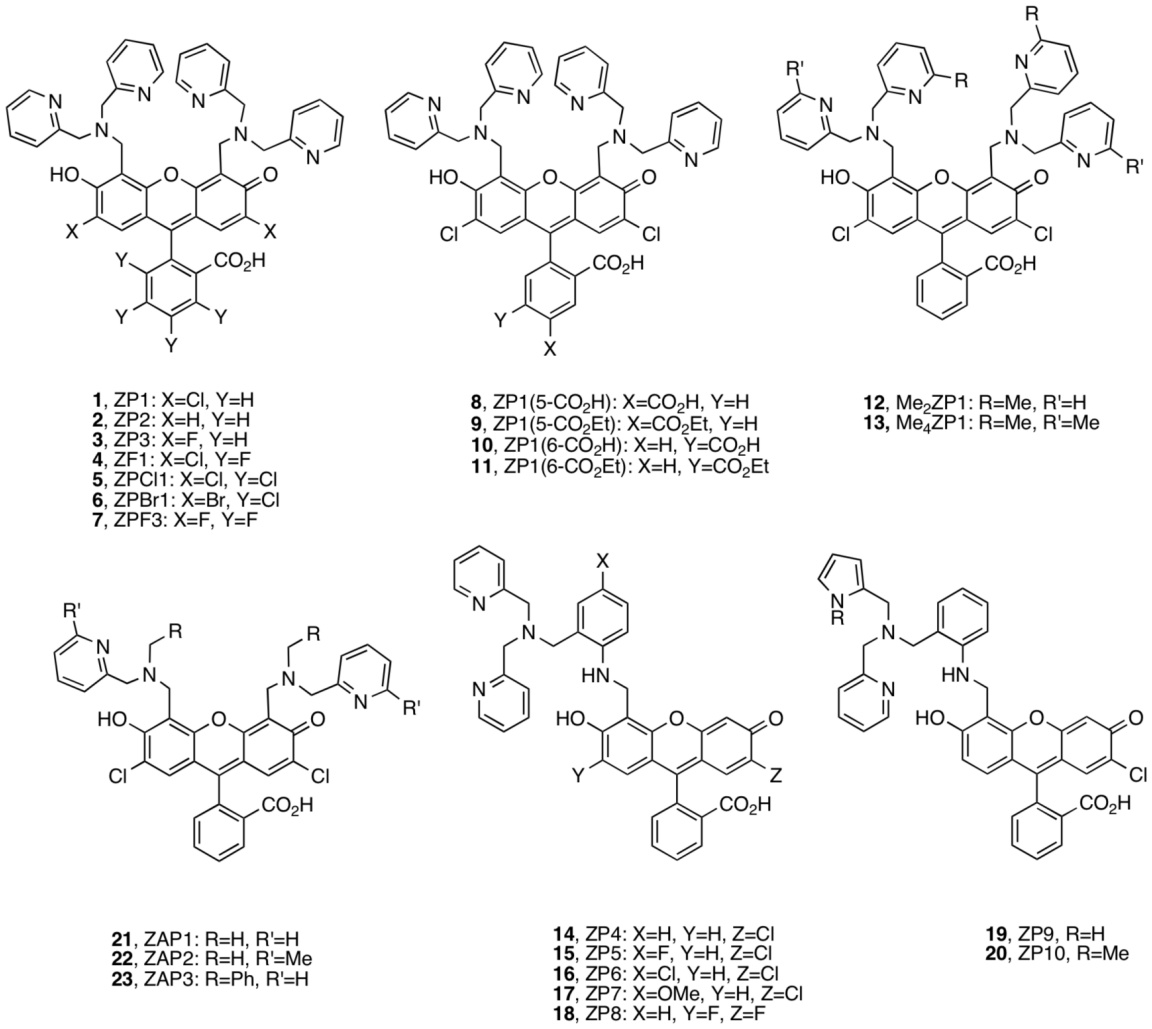

Figure 1.
Zinpyr and ZAP1-3.

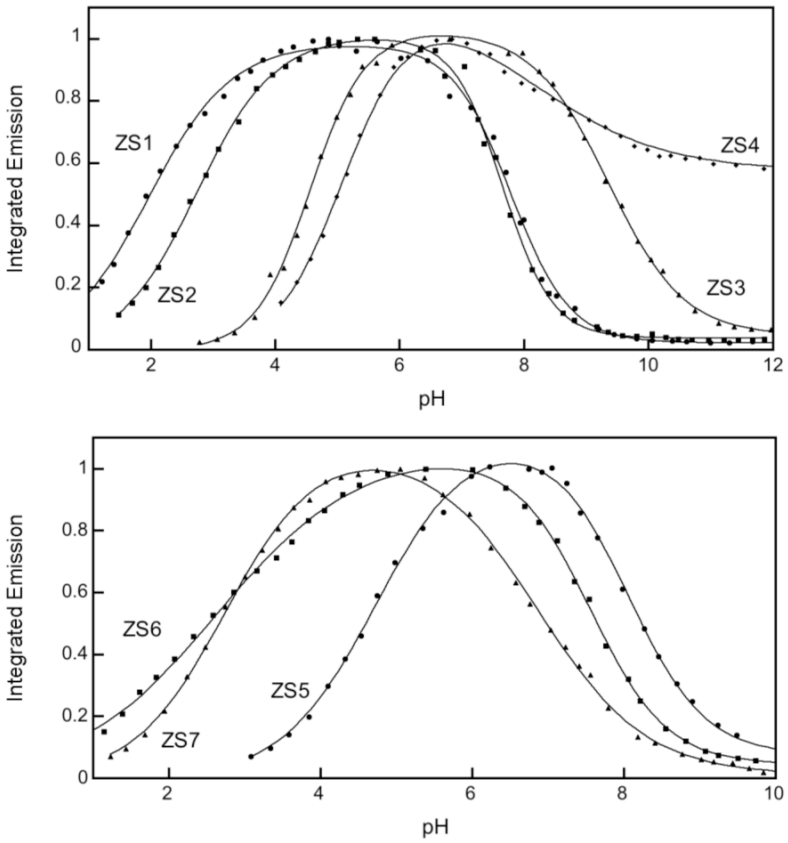

Figure 2.
Normalized pH-dependent fluorescence of representative ZS sensors (refs. 36, 37). Corresponding pK_a values are given in Table S1.

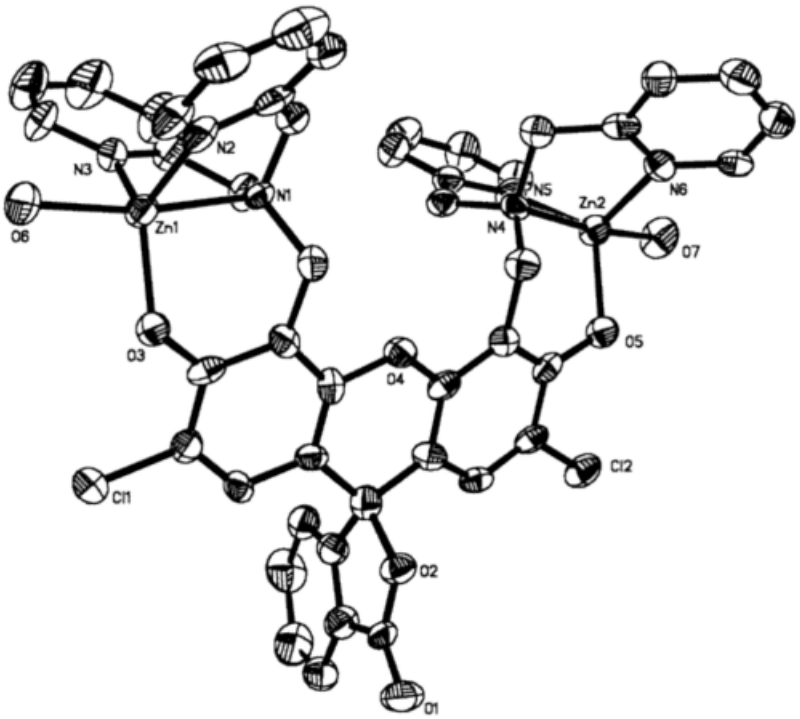

Figure 3.
Partial ORTEP diagram of $[Zn_2(ZP1)(H_2O)_2(ClO_4)_2]\cdot 6H_2O$ showing 50% thermal ellipsoids (ref. 22).

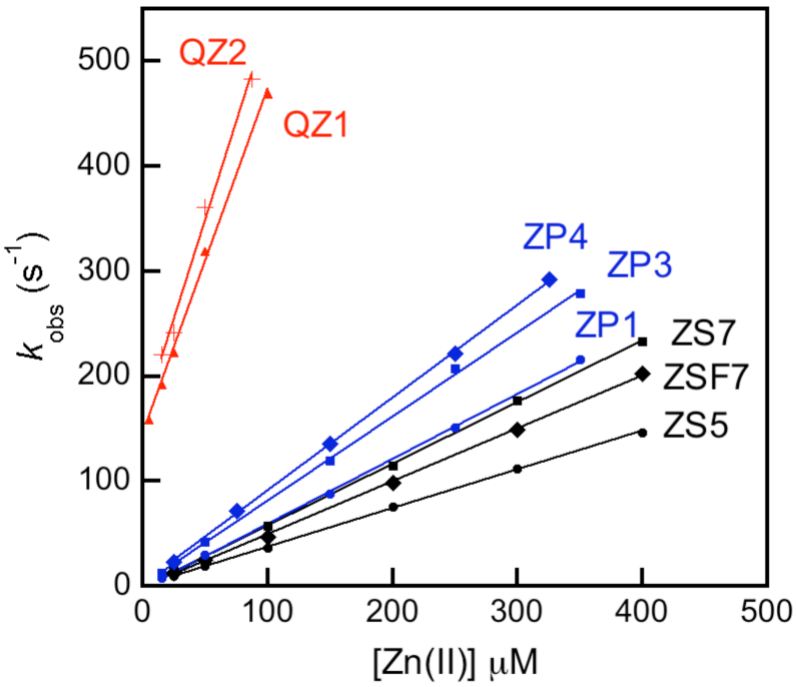

Figure 4.
Plots of k_{obs} vs. [Zn(II)] obtained by stopped-flow fluorescence studies for selected Zn(II) sensors. Table S2 contains the rate constants (refs. 33, [37]).

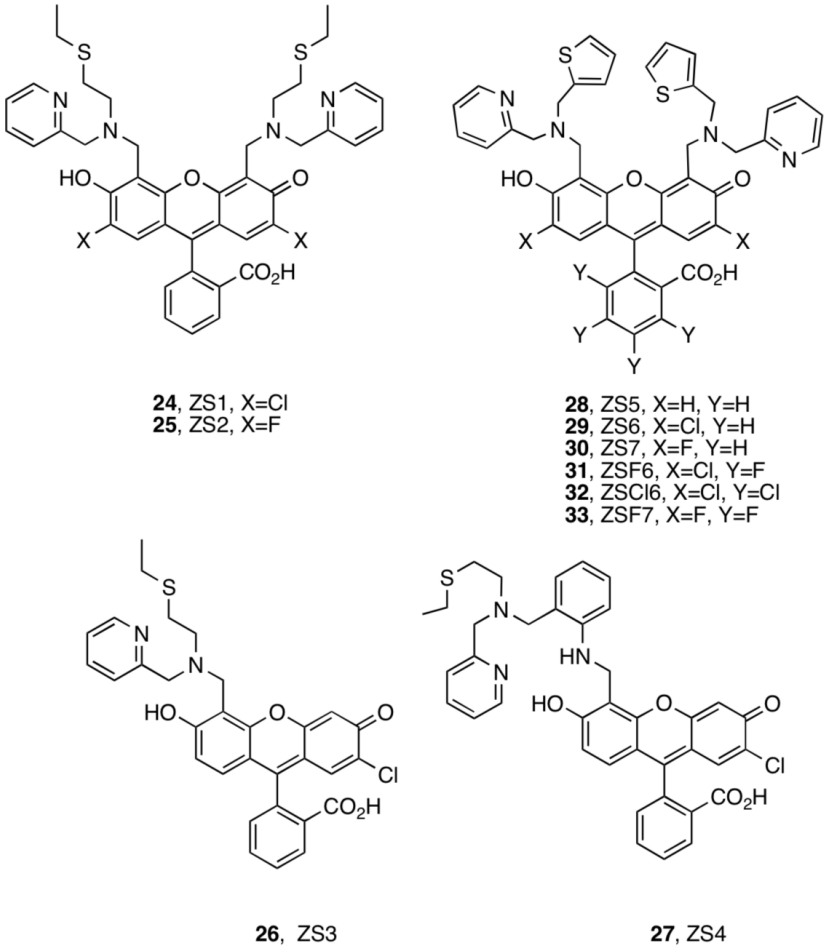

Figure 5.
Zinspy sensors.

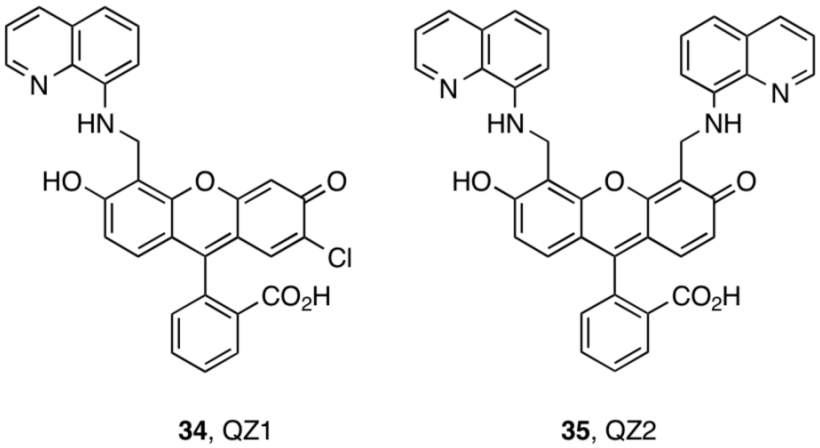

Figure 6.
QZ sensors.

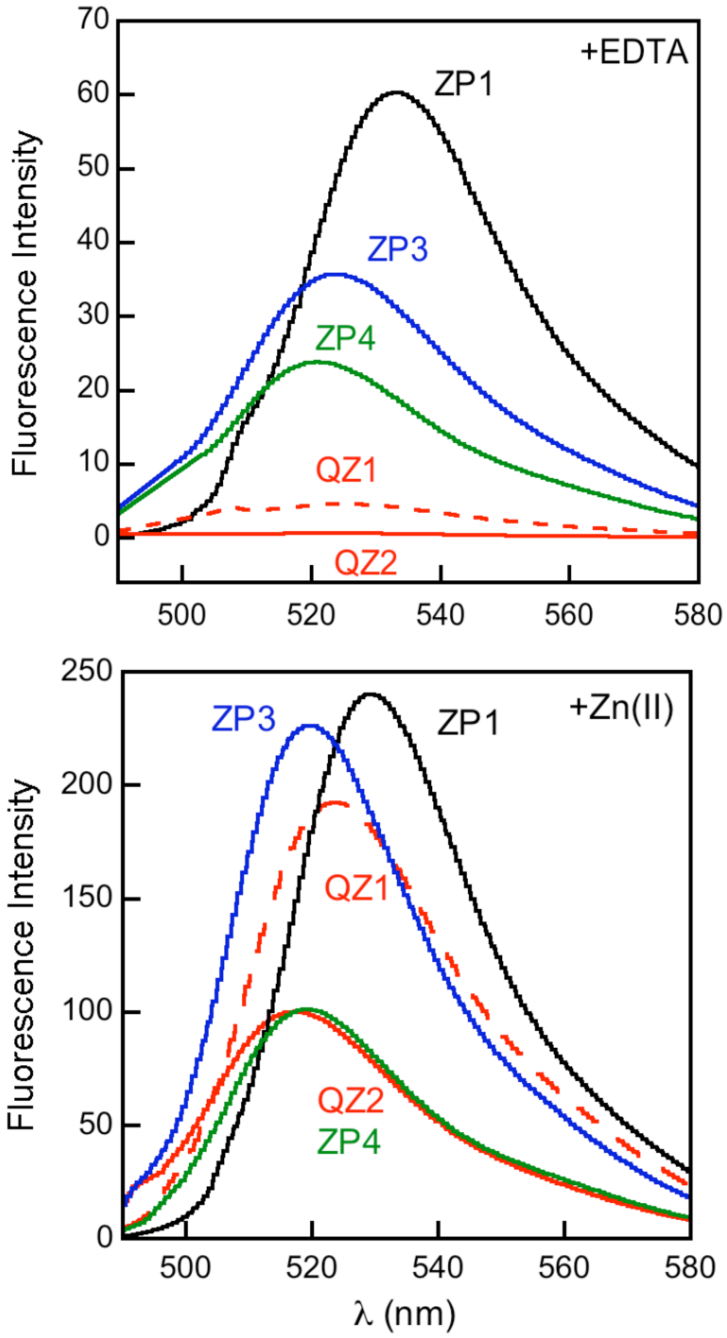

Figure 7.
Relative emission of metal-free and Zn(II)-saturated solutions of 1 μM sensor (pH 7) (ref 37).

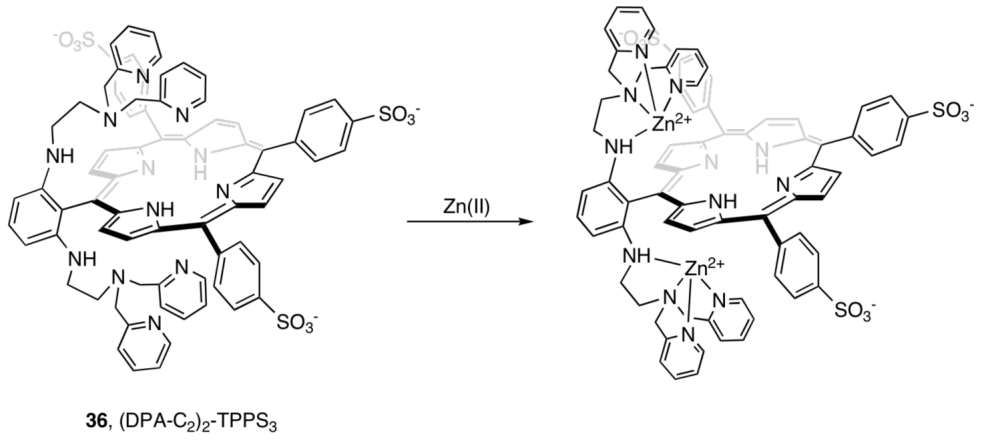

36, (DPA-C_2)$_2$-$TPPS_3$

Figure 8.
Sensor (DPA-C_2)$_2$-$TPPS_3$.

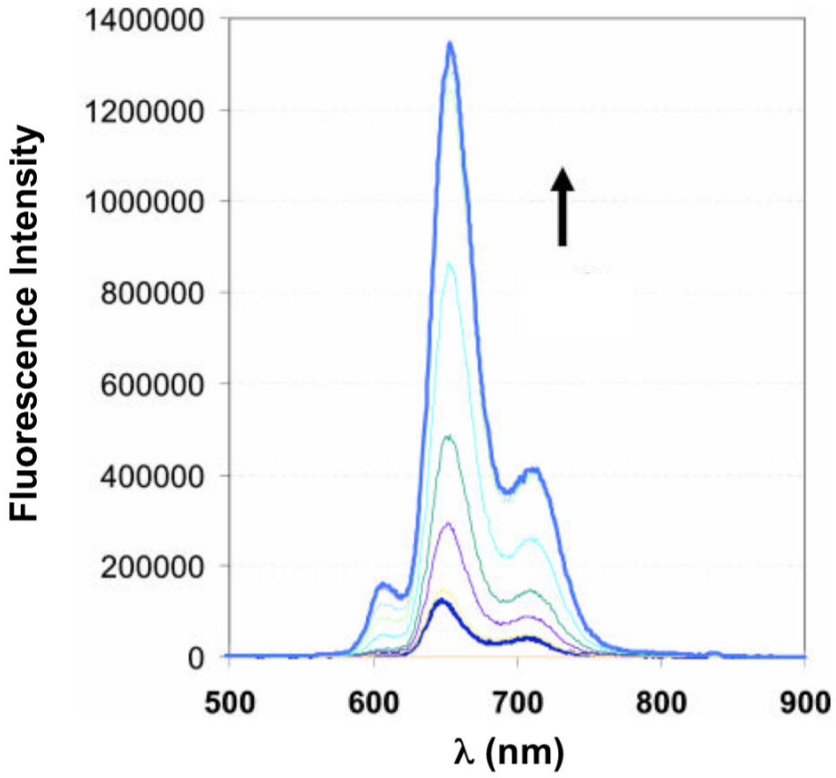

Figure 9.
Fluorescence response of 5 μM $(DPA\text{-}C_2)_2$-$TPPS_3$ to 0, 1, 2.5, 3.5, 5 (saturation point),7.5, 10 and 20 μM Zn(II) (pH 7) (ref. 41).

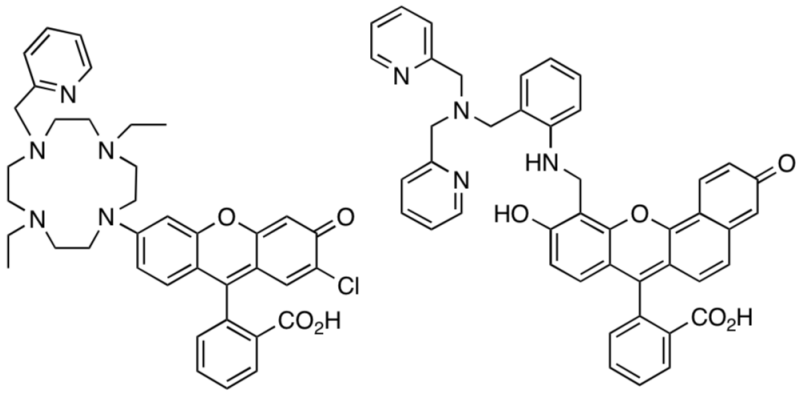

Figure 10.
RF2 and ZNP1.

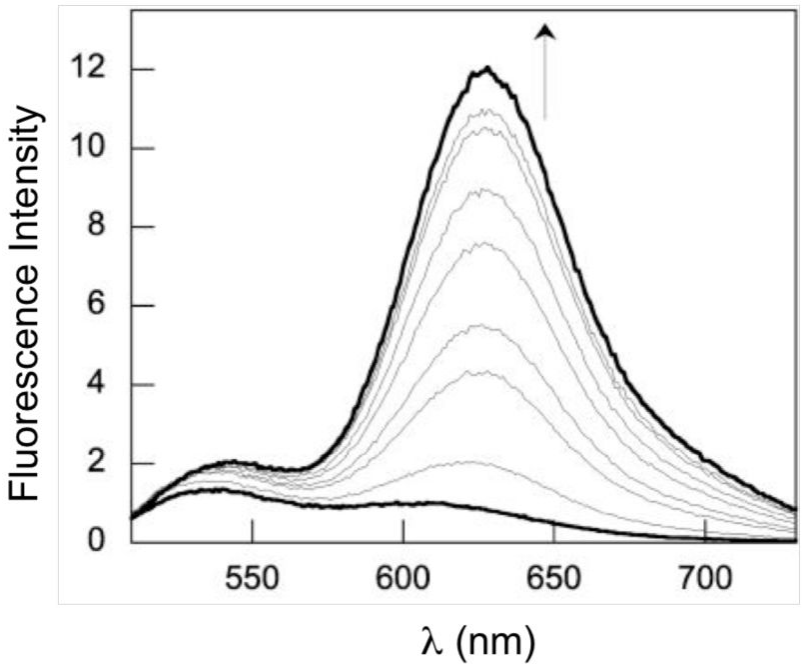

Figure 11.
Fluorescence response of 20 μM ZNP1 to 0, 0.17, 0.42, 0.79, 1.3, 2.1, 3.4, 5.6 and 10.2 nM (saturation point) Zn(II) (pH 7.5) (ref 44).

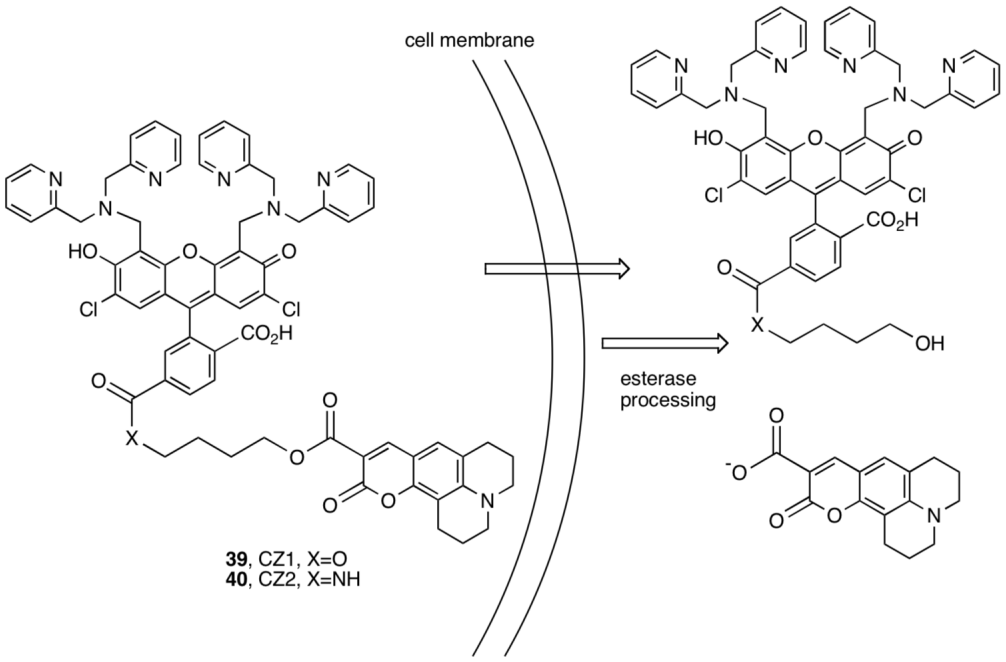

Figure 12.
Sensors CZ1 and CZ2.

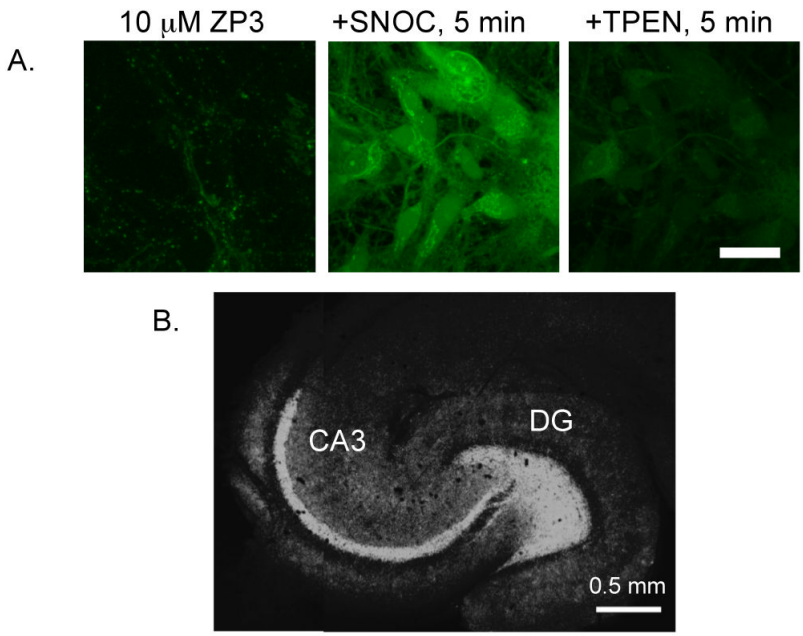

Figure 13.
(A) SNOC-induced release of endogenous Zn(II) in DG neurons detected by ZP3 (scale = 25 μm). TPEN addition reversed the fluorescence signal. (B) ZP3 staining of an acute hippocampal slice from an adult Sprague-Dawley rat (Nolan, Jaworski, Sheng, and Lippard, unpublished results).

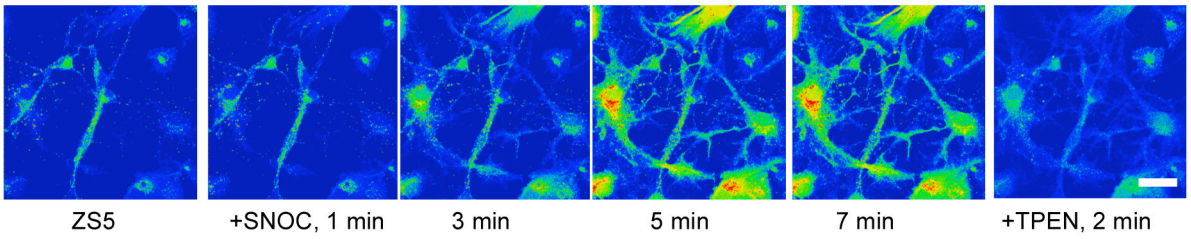

Figure 14.
(A) SNOC-induced release of endogenous Zn(II) in DG neurons detected with ZS5 (scale = 25 μm). TPEN addition reversed the fluorescence signal (ref. 37).

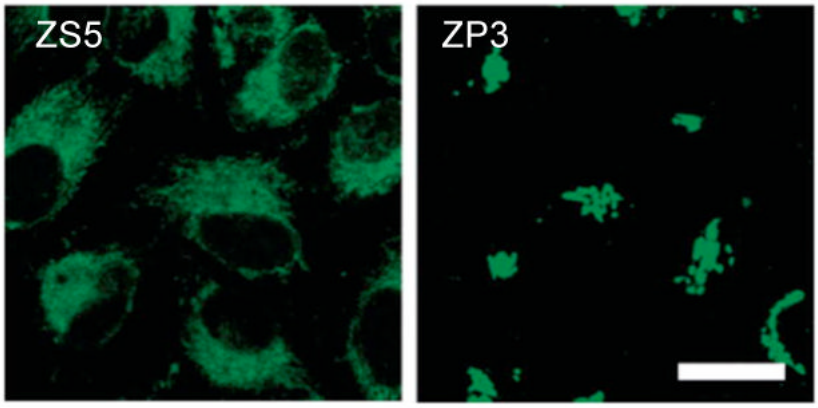

Figure 15.
Subcellular compartmentalization of ZS5 (left, mitochondrial) and ZP3 (right, Golgi) in HeLa cells (scale = 25 μm) (ref. 37).

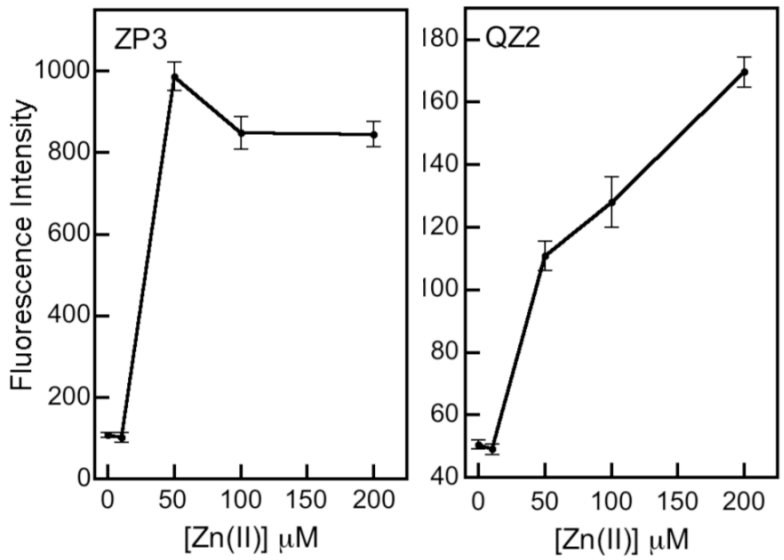

Figure 16.
Quantification of intracellular (HeLa) fluorescence from ZP3 and QZ2 following addition of 0 - 200 μM 10:2 Zn(II)/pyrithione (ref. 33).

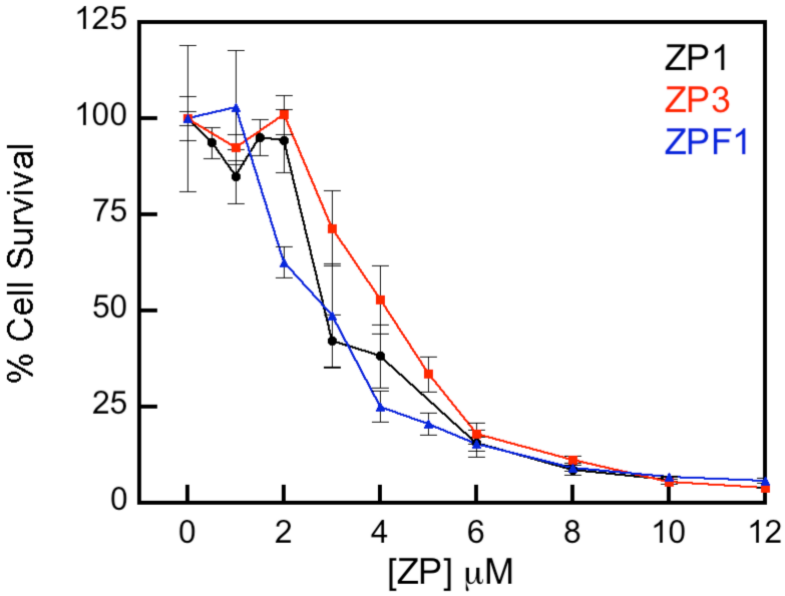

Figure 17.
Survival of HeLa cells treated with ZP and quantified by the MTT assay 5 days after treatment (Nolan and Lippard, unpublished results).